

## CIAT Research Online - Accepted Manuscript

---

### **A fuzzy logic slope-form system for predictive soil mapping of a landscape-scale area with strong relief conditions**

The International Center for Tropical Agriculture (CIAT) believes that open access contributes to its mission of reducing hunger and poverty, and improving human nutrition in the tropics through research aimed at increasing the eco-efficiency of agriculture.

CIAT is committed to creating and sharing knowledge and information openly and globally. We do this through collaborative research as well as through the open sharing of our data, tools, and publications.

**Citation:**

Bui, Le Vinh; Stahr, Karl; Clemens, Gerhard. 2017. A fuzzy logic slope-form system for predictive soil mapping of a landscape-scale area with strong relief conditions. *Catena* 155: 135-146.

**Publisher's DOI:**

<http://dx.doi.org/10.1016/j.catena.2017.03.001>

**Access through CIAT Research Online:**

<http://hdl.handle.net/10568/80475>

**Terms:**

© 2016. CIAT has provided you with this accepted manuscript in line with CIAT's open access policy and in accordance with the Publisher's policy on self-archiving.



This work is licensed under a [Creative Commons Attribution-NonCommercial-NoDerivatives 4.0 International License](https://creativecommons.org/licenses/by-nc-nd/4.0/). You may re-use or share this manuscript as long as you acknowledge the authors by citing the version of the record listed above. You may not change this manuscript in any way or use it commercially.

For more information, please contact CIAT Library at [CIAT-Library@cgiar.org](mailto:CIAT-Library@cgiar.org).

# 1 **A fuzzy logic slope-form system for predictive soil mapping of a** 2 **landscape-scale area with strong relief conditions**

3 Bui Le Vinh<sup>a,b,c\*</sup>, Karl Stahr<sup>b</sup>, Gerhard Clemens<sup>b</sup>

4 <sup>a</sup> Department of Land Management, Faculty of Land Management, Vietnam National University  
5 of Agriculture, Trau Quy, Gia Lam, Hanoi, Vietnam, email: [v.bui@cgiar.org](mailto:v.bui@cgiar.org),  
6 [bui\\_le\\_vinh@yahoo.com](mailto:bui_le_vinh@yahoo.com).

7 <sup>b</sup> Institute of Soil Science and Land Evaluation (310), University of Hohenheim, 70593 Stuttgart,  
8 Germany, email: [v.bui@cgiar.org](mailto:v.bui@cgiar.org), [bui\\_le\\_vinh@yahoo.com](mailto:bui_le_vinh@yahoo.com), [Karl.Stahr@uni-hohenheim.de](mailto:Karl.Stahr@uni-hohenheim.de),  
9 [GeCle@gmx.net](mailto:GeCle@gmx.net)

10 <sup>c</sup> International Center for Tropical Agriculture (CIAT), regional office for Asia, Institute of  
11 Agricultural Genetics, Km2 Pham Van Dong Street, Tu Liem, Hanoi, Vietnam, email:  
12 [v.bui@cgiar.org](mailto:v.bui@cgiar.org), [bui\\_le\\_vinh@yahoo.com](mailto:bui_le_vinh@yahoo.com).

13 \* Corresponding author. International Center for Tropical Agriculture (CIAT), regional office for  
14 Asia, Institute of Agricultural Genetics, Km2 Pham Van Dong Street, Tu Liem, Hanoi, Vietnam.  
15 Phone: +84 4 375 76969. Email: [v.bui@cgiar.org](mailto:v.bui@cgiar.org), [bui\\_le\\_vinh@yahoo.com](mailto:bui_le_vinh@yahoo.com) (L.V. Bui).

## 16 **Abstract**

17 We studied an improved slope form system using a fuzzy logic method to assess and map soil  
18 fertility of a mountain region in northern Vietnam that has strong relief conditions. The lack of  
19 good soil mapping techniques in Vietnam has brought about insufficient soil information, which  
20 often leads to false recommendations for land use and crop planning. The reviewed literature  
21 describes soil-mapping techniques using fuzzy logic method, but all of them are applied for  
22 mapping areas that have gentle relief conditions that are unlikely to be applicable to the  
23 mountainous soils in our study area. In this paper, we introduce a detailed slope form system that

24 significantly describes the complexity of terrain characteristics of the area to be mapped, and  
25 provides more detail about the variability of the soil fertility of the area. Nine basic slopeforms  
26 were used to characterize for each of upper-, middle-, and foot slope positions, making the list 27  
27 slopeforms. Together with crest and valley, the total unit number is 29. We investigated soils of  
28 the area and classified them into the major soil groups and calculated soil property indices for all  
29 of them. We identified four major environmental parameters affecting soil formation and soil  
30 quality: geology, elevation, slope inclination and land use. The findings indicated that soil fertility  
31 differs at slope positions. Soils located at upper slope positions, where agricultural activity only  
32 started recently, are more fertile than those found at middle slope positions. Soils located at foot  
33 slope positions, where eroded sediments accumulate, also have high levels of fertility compared to  
34 those on the middle slope. The improved slope form system then became an important additional  
35 environmental parameter for this soil mapping work. At a same comparable category, i.e. slope  
36 position, geology, soil group, elevation, slope gradient, straight slopeforms are an indicator for  
37 better soil fertility compared to convex and concave forms. Although the findings could not specify  
38 soil fertility variability for all 29 slopeforms, they did emphasize the major differences in soil  
39 fertility and soil formation based on three major forms of convex, straight and concave, with other  
40 factors taken into account, such as slope inclination, geology and elevation. We expect our results  
41 to be used by scientists and local authorities in deriving more effective land use and crop options  
42 for land use management strategies for the northern Vietnam's mountain regions.

43 *Keywords:* fuzzy logic, relief conditions, slopeform, slope position, soil mapping, soil fertility  
44 assessment

## 45 **1. Introduction**

46 The need for achieving spatial soil information and soil fertility details for research and  
47 development purposes has led to the generation of advanced soil mapping techniques (Zhu et al.,  
48 1996; Schuler, 2008; Qin et al., 2012). These techniques have been widely used in soil science for  
49 studying the spatial distribution of soils (Zhu, A.X., 1997a; Schuler et al., 2010), soil properties  
50 (Zhu et al., 1997b; Batjes, 2008; Qin et al., 2013), land evaluation and land-use planning  
51 (Herrmann et al., 2001), and soil and land health (Vågen and Winowiecki, 2012; Winowiecki et  
52 al., 2015). Fuzzy logic-based mapping techniques have long been applied for mapping spatial soil  
53 distribution and soil fertility studies (Burrough, 1989; McBratney et al., 2003; Zhu et al., 2010).  
54 The application of these techniques can be implemented in two approaches: data driven and  
55 knowledge-based (Zhu et al., 2010). The former is applied when there are sufficient data. The latter  
56 is normally used when there are not enough data for mapping soils of a larger area, for example at  
57 regional scale. In the latter case, when a large amount of field soil samples cannot be obtained to  
58 sufficiently map soils of a landscape-scale area, local soil experts are needed to describe  
59 knowledge on soil-environment relationship. To acquire this relationship, fuzzy membership  
60 functions defined by soil-environment relationships must be constructed to map spatial continuity  
61 of soils. Unique combinations of environmental variables characterize the formation of each soil  
62 group are obtained via various purposive soil sampling strategies (Bui et al., 1999; Qi and Zhu,  
63 2003).

64 One of the much studied environmental variables influencing soil occurrences is transitions among  
65 slope positions over landscape: the gradation of positions from crest, upper slope, middle slope,  
66 foot slope, to valley along a catena. This knowledge is very important in studying spatial  
67 distribution of soils with geomorphology-prone formation and especially soil fertility variability

68 across various slope positions. However, slope gradation has not been studied and quantified  
69 thoroughly for all geomorphological types, for example:

70 • Studies using crisp classification of slope positions (Young, 1972; Conacher and Dalrymple,  
71 1977; Speight, 1990) do not successfully depict the continuity of slope positions because they  
72 only assign binary values to map objects.

73 • Schuler et al. (2010) used a Maximum Likelihood approach to map a Thai region with strong  
74 relief conditions, but did not sufficiently capture effects of slopeforms on hillslopes (only  
75 identified convex, concave and linear forms) to formation of soils and their fertility variability.

76 • Qin et al. (2009) used fuzzy logic to derive nine gradual slope positions in studying spatial soil  
77 distribution and soil variability. However, this proved successfully only for an area of 60km<sup>2</sup>  
78 with gentle relief conditions (the lowest point of 233.6m asl and the highest point of 352.6m asl  
79 and average slope gradient of 2<sup>0</sup>).

80 Qin's slope gradation quantification technique was the inspiration to this study. However, the target  
81 area of Yen Chau district in the northern mountain region of Vietnam has stronger relief conditions  
82 than those of Qin's work. Yen Chau is characterized by steeper, longer and rougher slopes  
83 (elevation difference between the lowest and highest points is over 1400m and 60% total land falls  
84 into 9-35<sup>0</sup> slope gradient range). Therefore, to fully describe soil-slope gradation relationship in this  
85 specific study area required another way of quantifying slope positions.

86 This study aimed to develop a slopeform system that is detailed enough to study soil-environment  
87 relationship in an area, with the focus on the interrelation between soils and terrain morphology.

88 Firstly, five major slope positions for a single hillslope were generated: crest, upper, middle, foot  
89 slope, and valley. Peucker and Douglas' (1975) algorithm was applied to generate the highest  
90 (crest) and lowest (valley). The three mid-slope positions were generated using Skidmore's (1990)

91 Relative Position Index (PPI) algorithm. Secondly, the three major forms of convex, straight, and  
92 concave were used to characterize the three mid-slope positions, in both horizontal and vertical  
93 directions. Since these slope positions occupy most of the slope length, it was hypothesized that  
94 different detailed forms could lead to formation of certain soil groups and variability of soil fertility  
95 in the area to be mapped. The development of this detailed slopeform system applied fuzzy logic  
96 incorporated in SoLIMSolutions 2010 software upgraded by Zhu (2010).

## 97 **2. Material and methods**

### 98 *2.1. Study area and environmental setting*

99 A total area of 519 km<sup>2</sup> in the Yen Chau district of Son La province (Fig.1a) was mapped. Soils  
100 and soil fertility variations were mapped for the 193 km<sup>2</sup> of arable sloped land. Paddy rice fields  
101 were found in valleys along major rivers and streams, occupying 17km<sup>2</sup> and forests covered 262  
102 km<sup>2</sup>. The remaining 47 km<sup>2</sup> area was not of interest in this research.

103 The area has strong relief variations represented by a big difference between the highest (1567m  
104 asl) and the lowest (153m asl) elevation points (Fig.1b), with most of the long steep slopes found  
105 within the range of 9<sup>0</sup>-35<sup>0</sup>. The monsoonal climate is characterized by two distinctive seasons, a  
106 rainy season from May to October and a dry season from November to April of the next year. The  
107 statistics of Yen Chau weather station showed an annual average temperature of 24<sup>0</sup>C and  
108 precipitation of 1257mm (data of 2000-2007).

109 The geology (Fig.1c) is part of the larger Vạn Yên geology and minerals system (Bao, 2004), which  
110 consists of five major geological units: (1) Volcanic Magmatites (VO) including aphyric basalt,  
111 magnesium-high basalt, andesitobasalt, andesitodacite, trachyte, agglomerate, and tuffaceous  
112 sandstone; (2) Clastic Sediments (SC) including clay shale, marl, sericite schist, agglomerate,  
113 polymictic gritstone, sandstone, siltstone, and coal; (3) Yen Chau Formation–Lower Subformation

114 (K<sub>2</sub>yC<sub>1</sub>) including four members of conglomerate, gritstone, sandstone, and interbedding of  
115 chocolate claystone; (4) Yen Chau Formation–Upper Subformation (K<sub>2</sub>yC<sub>2</sub>) including two  
116 members of sandstone and interbedding of conglomerate; and (5) Limestone (SO). Information  
117 about alluvial and colluvial deposit units was initially not available. Their characteristics were only  
118 noticed during the soil surveys. Alluvial and colluvial deposits prevail at valleys and lower slopes,  
119 where alluvial deposits are found along stream banks at slopes that are 8% or less and within a  
120 radius of 100m from the banks. Colluvial deposits follow up to 16% slopes. The spatial delineation  
121 of these two new units on the geology map was derived in ArcGIS 9.3.

122 The major crops on the upland slopes are maize (*Zea mays L.*) and cassava (*Manihot esculenta C.*)  
123 (Clemens, et al., 2010; Häring et al., 2010), with the observed effective rooting depths being 0-  
124 30cm for cassava and 0-50cm for maize. There is only a small percentage (1.18%) of the natural  
125 land used for fruit trees, being located in home gardens and mainly at lower slope positions with  
126 moderate slope inclinations (Clemens et al., 2010).

## 127 **2.2. Sampling and soil characterization**

128 Farmers' knowledge about local soils, their distribution and fertility was studied (Clemens et al.,  
129 2010) to plan a field survey. The catena concept was applied to locate soil observations for soil  
130 investigation and sampling. Five soil profiles were minimally studied for one single slope covering  
131 five major slope positions: crest, upper, middle, foot slope, and valley. The mapping of five major  
132 slope positions (see details in 2.3.2) was based on Relative Position Index (RPI), DEM-derived  
133 profile and planform curvature parameters. Since soils at forested mountain tops were not studied,  
134 the crest position was eliminated and the upper slope position was determined right after the forest-  
135 field boundary. 110 soil profiles were investigated and sampled for the five major geological units

136 and the derived alluvial and colluvial deposits. The soil sampling was implemented by PhD, MSc,  
137 BSc, and internship students working in the Uplands Program during 2006–2012.

138 The soil profiles were dug down to the depth of 1.2–1.8m, then field described and classified  
139 according to FAO (2006) and the IUSS Working Group WRB (2006). The description and  
140 sampling were made for every soil horizon. The soil physical and chemical properties used in this  
141 study were the same like Clemens et al. (2010).

142 For soil fertility control, further calculations of soil properties were carried out for the calibration  
143 of the soil fertility mapping model. These calculations were made for the effective rooting space  
144 (ERS, dm), which is defined as the maximum depth of water, that can be reached by the roots  
145 during years of low rainfall (FAO, 2006). In this study, the ERS was taken down to 70cm and was  
146 separated into topsoil (0–30cm) and subsoil (30–70cm) to highlight the higher root densities and  
147 soil nutrient stocks in the topsoil to the subsoil (Clemens et al., 2010). These further soil properties  
148 computed based on Jahn et al. (2003) for every soil horizon are as follows:

149 (i) *Physical properties*: Soil volume ( $l/m^2$ ) was the function of soil thickness (dm) and stone  
150 content (%). Soil mass ( $kg/m^2$ ) is the total weight of soil material in a volumetric unit and was  
151 calculated on the function of soil volume and bulk density (BD) multiplied factor 1 for the  
152 topsoil and factor 0.5 for the subsoil. It is more compacted in the subsoil, which makes the soil  
153 mass of the subsoil a lot higher than that of the topsoil for a same soil depth. The factor 0.5 is  
154 used to equalize soil mass of the subsoil with that of the topsoil. Air capacity (AC) and  
155 available water capacity (AWC) ( $l/m^2$ ) were the functions of estimated AC (%) and AWC (%)  
156 with soil volume.

157 (ii) *Chemical properties*: S-value ( $mol/m^2$ ) was the function of effective cation exchange capacity  
158 ( $CEC_{eff}$ ) and base saturation (BS). The  $CEC_{eff}$  was estimated based on Jahn et al. (2006). S-



159 value was multiplied with factor 1 for the topsoil and 0.5 for the subsoil. The use of factor 0.5  
160 is the same as explained in (i). The range-standardized sum parameter (N-P-S) proposed by  
161 Mausbach and Seybold (1998) was used to quantify soil fertility. This parameter is the sum of  
162 the stocks of total nitrogen ( $N_t$ ), available phosphorus ( $P_{\text{Bray1}}$ ), and S-value and was applied in  
163 this research in continuation of the work of Clemens et al (2010). These three stock values  
164 were standardized by setting the maximum value to 1 and the minimum value to 0 of each of  
165 the three parameters for the whole set of soil profiles and the values in between were calculated.  
166 The sum parameter N-P-S was achieved by summing up the 3 standardized values of N, P, and  
167 S-value. The parameter N-P-S, therefore, has the value range from 0 to 3.

### 168 ***2.3. Construction of the system of 29 slopeforms***

#### 169 *2.3.1. Generation of a digital elevation model (DEM) for the study area*

170 The DEM of the study area was constructed from vector files of contour lines, rivers and streams,  
171 the border of the study area, and elevation points using Topo to raster tool in ArcGIS 9.3. The map  
172 scale was 1:25,000 and the map resolution was set to be 10m by 10m. The output was a raster file  
173 as can be seen in Fig.1b. This DEM file was an important data type that was later used to extract  
174 other types of data for deriving slopeforms such as curvatures, relative position index (RPI), slope  
175 positions, and those as input parameters for the predictive soil mapping models such as slope  
176 inclination and slope aspect.

#### 177 *2.3.2. Generation of five major slope positions*

178 The method for generating five major slope positions was well explained in Skidmore (1990).  
179 Firstly, the DEM was used to extract a crest and a valley to identify the highest and lowest points  
180 of a single slope applying Peucker and Douglas (1975) algorithm in SimDTA software (Qin et al.,  
181 2009). Secondly, the middle slope positions were interpolated applying the Relative Position Index

182 (RPI) as defined in Skidmore (1990). The value range of RPI is [0,1] with 0 being a valley and 1  
183 being a ridge. This value range is subdivided to describe the five major slope positions for the area:  
184 ridge [0.99, 1], upper slope [0.7, 0.99], middle slope [0.3, 0.7], foot slope [0.01, 0.3], and valley [0,  
185 0.01].

### 186 *2.3.3. Generation of the detailed system of 29 slopeforms*

187 Nine basic slopeforms defined in FAO (2006) were derived for each of upper, middle, and foot  
188 slope positions, making up to 27 slopeforms for this long slope range and totally 29 forms from  
189 crest to valley. Profile and planform curvature parameters were derived from the DEM using  
190 ArcGIS 9.3 to determine vertical and horizontal shapes of the 27 slopeforms. Profile curvature is  
191 parallel to the slope and indicates the direction of maximum slope and is the rate of change of  
192 gradient. It affects the acceleration and deceleration of flow across the surface and hence influences  
193 soil aggradation or degradation. Planform curvature is defined as the rate of change of aspect being  
194 perpendicular to the direction of the maximum slope and affects the convergence and divergence  
195 of flow across the surface (Odeh et al., 1991).

196 Three major forms for each of these parameters were: convex, straight, and concave. The  
197 parameter values set for these three major forms both vertically and horizontally were: convex >  
198 0.005, straight [-0.005, 0.005], and concave < -0.005. The selection of these values was validated  
199 with field check to best describe gradual changes of slopeforms along a slope. The 29 slopeforms  
200 were assigned with values of RPI, profile and planform curvatures as indicated in Table 1.  
201 Mapping of this slopeform system was achieved by applying SoLIMSolutions 2010 software (Zhu  
202 et al., 2010).

### 203 *2.4. Structural organization of the soil database*

204 The soil database structure was developed based on the characterization of terrain characteristics of  
205 the study area. First, terrain units of the area were studied. According to Van Engelen and Wen  
206 (1995), terrain units are the general description of physiography and parent material. Three major  
207 landforms, level (L, inclination<8%), sloped land (S,  $8 \leq \text{inclination} < 30\%$ ), and steep land (T,  
208 inclination>30%), defined by Cong (2011) for a subcatchment scale of Yen Chau were used to  
209 classify subdivided landforms in this study. There were three subunits for L: L<sub>1</sub> (0-2%), L<sub>2</sub> (2-4%),  
210 L<sub>3</sub> (4-8%); two for S: S<sub>1</sub> (8-16%) and S<sub>2</sub> (16-30%); and six for T: T<sub>1</sub> (30-50%), T<sub>2</sub> (50-60%), T<sub>3</sub> (60-  
211 70%), T<sub>4</sub> (70-84%), T<sub>5</sub> (84-100%), and T<sub>6</sub> (>100%), totaling 11 subdivided landforms. The slope  
212 parameter was converted from degree to percentage on which the database of this study was built.  
213 These 11 subdivided landforms were merged with the 5 geological units to derive a map of 55 terrain  
214 units. Alluvial and colluvial deposits remain as two independent terrain units, totally making up 57  
215 terrain units for the study area. Given the minor impact of slopeforms as well as the latter 2 terrain  
216 units to soil formation and fertility at crest and valley, the occurrences of soils and soil fertility  
217 variability were studied on the 55 terrain units and 27 slopeforms, i.e. 1485 components. The fact  
218 that only 88 soil components from 110 soil profiles were identified would largely influence the  
219 quality of this work. To support calibration of the model, we used a reasoning method (section 3.1)  
220 built on knowledge from 11 junior and senior soil scientists working in the project to fill in the gaps  
221 of missing information. The team commonly agreed that only major slopeforms (straight, concave  
222 and convex) in combination with slope gradient had significant influences to soil occurrences and  
223 fertility dynamics (section 5.3).

224 Environmental parameters were collected for each of the soil profiles in which the slopeform and  
225 slope position of a profile were taken from the achieved slopeform map. Table 2 is a structural  
226 example of the soil database constructed for subdivided landforms T<sub>1</sub> and T<sub>2</sub>. The soil database for

227 the other subdivided landforms was organized the same way. Other parameters, such as slope aspect,  
228 elevation, were entered in a detailed Excel soil data table.

### 229 ***2.5. Predictive soil mapping under fuzzy logic***

230 The application of fuzzy logic theory in predictive soil mapping techniques have been very well  
231 explained in numerous publications and studies (Burrough, 1996; Yang et al., 2007; Zhu et al.,  
232 2010). This part only summarizes the fuzzy logic method for predictive mapping of soils and soil  
233 fertility indices with the emphasis on a slopeform system relevantly derived for the study area.

#### 234 *2.5.1. Constructions of fuzzy similarity functions*

235 The inference engine in SoLIM is operated using a raster data approach in which fuzzy similarity  
236 values (to values of prescribed soils) are calculated for every grid cell. The similarity value ranges  
237 from 0 (meaning the soil at a pixel is very different from a prescribed soil) to 1.0 (meaning the soil  
238 at a pixel carries exactly the same properties of the prescribed soil). The fuzzy minimum operator  
239 is used to calculate fuzzy membership values, or similarity values, (Zhu et al., 1996) for all map  
240 pixels of prescribed soils, and is expressed in equation 1. The intersection of sets  $A \in X$  and  $O \in X$   
241 which corresponds to the connective “and”, and its membership functions is given by:

$$\mu_N(x) = \min\{\mu_A(x), \mu_O(x)\}, x \in X \quad (1)$$

242 where  $x$  is an object which belongs to the set of object  $X$ ,  $\mu_A(x)$  is called the degree of membership  
243 of  $x$  in  $A$  which maps  $X$  to the membership space  $M$  (when  $M$  contains only the two points 0 and 1,  
244 and  $\mu_A(x)$  is identical to the characteristic function of a non-fuzzy set).

245 Environmental variables in one unique combination (soil instance) to a specific soil group are  
246 calculated with optimality values using three optimality curves: bell, S, and Z shapes (Zhu, 1999)  
247 as can be seen in Fig.2. Equation (1) is applied on these optimality values to derive the similarity  
248 value for a given map pixel. The set of environmental variables is used again for other soil instances

249 of this soil type for calculating optimality and similarity values. For example, Luvisols in Yen Chau  
250 can either be found on limestone with elevation from 300 m to 900 m a.s.l and with slope inclination  
251 below 30% at all slopeforms (instance 1) or limestone with elevation from 900 m to 1000 m a.s.l and  
252 slope inclination between 30% and 50% at slopeforms of 6, 15 and 24 (instance 2). After instances  
253 of this soil type are studied, the fuzzy maximum operator (equation 2) is applied to finalize the  
254 membership value of a map pixel for this soil type from the calculated membership values of the soil  
255 instances. For example, the similarity value of instance 1 is greater than that of instance 2, therefore,  
256 it better represents the similarity of Luvisols at this specific map pixel.

$$\mu_N(x) = \max\{\mu_A(x), \mu_O(x)\}, x \in X \quad (2)$$

257 This process goes on to other cells until it completes computing for all of the pixels of the study  
258 area. At this point, a thematic similarity map is produced for a single soil group. The engine then  
259 moves on to calculate for the rest of the prescribed soil types and more similarity maps are created.  
260 Finally, SoLIM can technically merge these similarity maps into one map, which assigns each cell  
261 with a value of one prescribed soil group based on the highest similarity value to this group using  
262 Hardened Map function in SoLIM. The final map is the soil/soil fertility map that delineates the  
263 spatial distribution of all soil/soil fertility groups for the mapping area.

#### 264 2.5.2. *Soil and soil fertility mapping*

265 Reference soil groups (RSGs) need to be described and classified according to FAO (2006) for all  
266 geological units and elevation ranges in the area through a collection of visited soil profiles. For all  
267 soil profiles studied, information of rock type, elevation, slope gradient, slope position, slopeform,  
268 slope aspect, land use type, cultivation period need to be collected to learn the relationship between  
269 their formation and fertility variability with the above environmental parameters.

270 Each of the major RSGs is then further classified into one or more soil subunits using prefix and  
271 suffix qualifiers in WRB (2006) to highlight soil property differences within a RSG. Major  
272 properties are identified for major RSGs, such as Alisols, Luvisols, Cambisols, etc., for most  
273 representative environmental parameters, such as Cutanic for a high clay content, Leptic for high  
274 a stone content of soils at slopes greater than 60%, Humic for soils found at upper slope positions  
275 where landuse after deforestation is younger and OM contents thus higher, Profondic for soils with  
276 an argic horizon having a clay content not decrease by 25 percent or more 150cm from the surface,  
277 etc. Information occurring these soil subunits is collected in Table 4 and calibrated in SoLIM to  
278 derive a soil subunit map for all major RSGs. This can be easily done based on the described soil  
279 profiles in the soil data set made for all RSGs that were contributed by all soil scientists working  
280 in the project, which will help provide a more diverse picture of soil distribution in the area.

281 To prepare for the soil fertility mapping model, soil fertility classes are defined based on calculated  
282 N-P-S values (Table 5). These fertility classes are then prescribed based on distinctive  
283 combinations of environmental parameters (same with the ones that were used in the RSG mapping  
284 model) as soil forming factors (see example in Table 6). The soil fertility classification is made for  
285 Alisols, Luvisols, Cambisols, Regosols, Leptosols, Fluvisols, Stagnosols, and Vertisols.

### 286 **3. Results**

#### 287 ***3.1. Mapping of the reference soil groups***

288 The soil investigation over the period 2006-2012 resulted in 11 RSGs, in which Alisols and  
289 Luvisols were the two most abundant RSGs and found on all rock types with 46 and 36 profiles,  
290 respectively. There were 7 Anthrosols, 7 Regosols, 4 Stagnosols, 3 Vertisols, 2 Cambisols, 2  
291 Phaeozems, 1 Leptosol, 1 Gleysol, and 1 Fluvisol. The fact that the total 110 soil profiles did not  
292 cover all combinations of relief parameters led to the use a reasoning strategy using expert

293 knowledge of the soil scientists working in the project. Field observations and personal  
294 impressions of soil formation in Yen Chau of junior and senior soil scientists working in the SFB  
295 564 project were gathered to estimate soil occurrences in empty relief combinations. This local  
296 soil expert then helped fill in the soil formation reasoning table (Table 3).

297 SoLIM, which is an automated soil inference system that studies the relationship between soils  
298 and environmental conditions, was used to generate fuzzy similarity maps (Zhu et al., 2010).

299 Eleven fuzzy similarity maps were derived for the study area with each map representing one RSG.

300 A hardened RSG map for the study area was derived from the fuzzy similarity maps (Fig.3). The

301 statistic results show that Alisols and Luvisols are the most abundant soil groups within the focal

302 mapping area, occupying 47.2% and 38.5% of the total area, respectively. Cambisols are the third

303 abundant soil group with 10.6% of the total area, which prevail at non-forested crest positions,

304 middle slope positions having convex slopeforms, and colluvial deposits at foot slope positions.

305 Leptosols, Regosols, Fluvisols, Stagnosols, and Vertisols have remarkably small areas with 1.8,

306 1.4, 0.4, 0.1, and 0.02% of the focal mapping area, respectively. The predicted occurrence of

307 Phaeozems spreads over a large area of 54 km<sup>2</sup> and paddy soils (Anthrosols and Gleysols) occupy

308 an area of 17 km<sup>2</sup>. However, these three RSGs were not evaluated with accurate assessment of

309 their occurrences and fertility because they are located outside of the area of interest as mentioned

310 before, i.e. arable sloped land or the focal mapping area.

311 Since the RSGs within the focal mapping area are only major soil groups and each group can have

312 a wide range of soil property values, evaluation of the results needed more detailed information.

313 Indirect assessment (Zhu et al., 2010) of this predictive soil mapping approach was, therefore,

314 necessary. To support this, a soil subunit map and a soil fertility map were derived for more diverse

315 evaluations.

### 316 **3.2. Soil subunit map**

317 Fig.3 shows the spatial distribution of 18 soil subunits of major RSGs. Alisols, Luvisols, and  
318 Cambisols had the most subunits (12/18) and together accounted for 95.8% of the predicted soil  
319 map. Cutanic is the most prominent property for Alisols and Luvisols in Yen Chau (Fig.4). Soils  
320 found at crest and high upper slope positions had higher amounts of organic matter than those at  
321 the lower positions, which resulted in a Humic property for Alisols, Luvisols and Cambisols at  
322 these locations. Within the middle slope length, Profondic is the major property at lower upper  
323 and higher middle slope positions, Leptic at the middle position having convex forms, equivalent  
324 to a high rock content, and Siltic at lower middle slope for both Alisols and Luvisols. Many  
325 Luvisols found had a Nitic property at lower middle and higher foot slope positions. Investigated  
326 Cambisols had a Dystric property at middle slope positions that have the concave-convex (CV)  
327 form, where topsoils were eroded and unconsolidated materials remained right before the bed rock.  
328 Cambisols found at foot slope positions mainly had a Luvic property for having deposition of  
329 eroded materials from upper slopes right on top of an in-situ argic horizon.

330 Each of the other RSGs (Regosols, Leptosols, Fluvisols, Stagnosols, and Vertisols) had one most  
331 representative subunit.

### 332 **3.3. Soil fertility map**

333 A detailed classification of 17 soil fertility classes was generated to see whether there would be  
334 some influence degree of the environmental parameters to soil fertility at this detail level (Fig.7  
335 a&b). Insignificance degrees resulted in the merging of them into four groups: good, moderate,  
336 low, and very low based on comparisons with soil properties calculated for all soil profiles and on  
337 information collected at all observation points. The good group included classes 1-4, covering an  
338 area of 35.5km<sup>2</sup> or 18.4% of the arable sloped land. The moderate group included classes 5-8,



339 occupying an area of 86.3km<sup>2</sup> or 44.7% of the arable sloped land. The classes 9-12 constituted the  
340 low fertility group, which occupied 66.4km<sup>2</sup> or 34.4% of the arable sloped land. The very low  
341 group was the smallest one spreading over an area of 4.8km<sup>2</sup> or 2.5% of the arable sloped land and  
342 merged from classes 13-17 (Fig.5b).

#### 343 **4. Validation of the soil, soil subunit and soil fertility maps**

344 Fifty extra soil profiles were described and classified using the WRB 2006 to evaluate the match  
345 of the observed soil data with the three predicted maps (Fig.7). The sampling strategy was  
346 purposive following the catenary sequences for the predictive soil map of Yen Chau focusing on  
347 crest, upper, middle-, and foot slope positions. Out of 50 validation points, 10 points were collected  
348 for VO, 9 for SO, 10 for SC, 12 for K<sub>2</sub>yC<sub>1</sub>, and 9 for K<sub>2</sub>yC<sub>2</sub>.

##### 349 ***4.1. Validation of the soil map***

350 Matching the validation points with the predicted RSG map showed an accuracy of 90% (a match  
351 of 9/10 points) for VO, 78% (7/9 points) for SO, 60% for SC (6/10 points), 67% (8/12 points) for  
352 K<sub>2</sub>yC<sub>1</sub>, and 88.9% (8/9 points) for K<sub>2</sub>yC<sub>2</sub>. Overall, 37 out of 50 observation points matched with  
353 the inferred RSG map, resulting in an accuracy of 76%. Compared to the results of different  
354 predictive soil mapping studies applying different methods, (Zhu et al., 1996; Zhu et al., 2010;  
355 Schuler et al., 2010) this accuracy is acceptable. It shows the consideration of slope positions and  
356 slopeforms in the soil-landscape relationships is useful in capturing a large portion of RSGs for  
357 this area of strong relief conditions in the NW Vietnam.

##### 358 ***4.2. Validation of the soil subunit map***

359 The 50 validation soil profiles were classified with soil subunits according to WRB (2006) to  
360 validate the results of the predicted soil subunit map. Matching the validation points with the soil  
361 subunit map showed an accuracy of 80% (a match of 8/10 points) for VO, 78% (7/9 points) for

362 SO, 60% for SC (6/10 points), 67% (8/12 points) for K<sub>2</sub>yC<sub>1</sub>, and 78% (7/9 points) for K<sub>2</sub>yC<sub>2</sub>. The  
363 overall accuracy of the soil subunit map was 72%, i.e. 36 out of 50 observation points matched  
364 with the inferred soil subunit map. This accuracy degree is still acceptable, which shows the ability  
365 of the model to capture most of the soil subunits identified for the area.

#### 366 ***4.3. Validation of the soil fertility map***

367 To validate the predicted soil fertility map (with 17 fertility classes), the same 50 validation data  
368 points and two indices applied in Zhu et al. (2010) were used: root mean square error (RMSE) and  
369 agreement coefficient (AC). The AC index was defined by Willmott (1984) as follows:

$$370 \quad AC = 1 - \frac{n * RMSE^2}{PE} \quad (3)$$

371

372 The sum parameter N-P-S was calculated for all of the 50 validation data points, resulting in 50  
373 observed N-P-S values. The locations of these observed values on the soil fertility map were used  
374 to extract the 50 corresponding predicted values. The RMSE the 50 data points from the predicted  
375 map is 0.58. For the N-P-S data value range from 0 to 3, this RMSE value is rather a big value,  
376 which shows quite distant differences between the predicted and observed values. The calculation  
377 of the AC index, which is 0.60, also confirmed a medium agreement (or an average match) between  
378 the predicted and the observed values at these 50 locations. This medium accuracy value means  
379 that the environmental parameters taken were not sufficient to achieve a better match between the  
380 predicted soil fertility map and the real fertility variations of soils in the mapping area. This result  
381 suggests that more parameters be used in order to improve the certainty of the inference result of  
382 the soil fertility map. For example, land-use history must have had lots of impact on soil fertility  
383 decline over time and, therefore, the fertility of soils at various locations that have different land-

384 use ages after deforestation. However, this parameter was not incorporated in the model due to the  
385 large size of the area to be mapped and the program's limited budget.

## 386 **5. Discussion**

387 Soil = (Cl, Pm, Og, Tp) t (Jenny, 1941) is a function to conceptualize the soil-environmental  
388 relationship, which states that the formation of soils (s) is influenced by different factors,  
389 remarkably climate (Cl), parent material (Pm), organisms (Og), and topography (Tp). These  
390 factors evolve with factor time (t). In this study, soil formation and soil fertility variability  
391 represented by SOM stocks follow the same rule and soil-forming factors are discussed in the order  
392 of importance.

### 393 **5.1. Parent material**

394 The study agrees with that of Schuler (2008), Parton et al. (1987) and Six et al. (2002) on different  
395 parent rocks resulting in the formation of different major soils determined by soil compositional  
396 properties, such as soil pH, clay content, CEC and BS; and by soil organic matter (SOM) whose  
397 stability and dynamics are very much controlled by clay content. In Fig.6, light clay composition  
398 in SC, i.e. sandy clay to clay loam in the topsoil and sandy clay loam to light clay in the subsoil,  
399 is the reason for having BS smaller than 50% in all soil profiles, which explains the absence of  
400 Luvisols and lower stocks of bases. Luvisols were found in all of the other four rock types. VO  
401 has highest BS, CEC and S-value values among all rock types due to having high clay contents:  
402 clay loam in the topsoil and clay in the subsoil, which is the reason for having Luvisols as the  
403 major soil, not Alisols. Both Luvisols and Alisols were found on SO, SC and K<sub>2</sub>yC<sub>2</sub>, in which  
404 average BS, CEC and S-value were highest in SO and lowest in SC.  
405 SOM contents were found to be higher in SC, VO and SO and lowest in K<sub>2</sub>yC<sub>1</sub>. The finding agrees  
406 with that of Clemens et al. (2010) which found the lowest average clay content of soils in K<sub>2</sub>yC<sub>1</sub>.

407 However, the SOM content rather depends largely on land-use history. Clemens et al. (2010) and  
408 Häring et al. (2010) found that soils developed in valleys of K<sub>2</sub>yC<sub>1</sub> and K<sub>2</sub>yC<sub>2</sub> had lower average  
409 SOM contents. Participatory investigations for land-use history in Yen Chau revealed that K<sub>2</sub>yC<sub>1</sub>  
410 and K<sub>2</sub>yC<sub>2</sub> soils have had longer cultivation periods for better access and denser population.

### 411 ***5.2. Climate in association with elevation***

412 The study coincides with that of Schuler (2008) that Luvisols prevail at elevations below 900m  
413 asl. Alisols are the major soil group above this line. The transition of Alisols to Luvisols in rising  
414 elevation is explained by elevation-triggered differences in temperature and rainfall. The higher  
415 temperature and more seasonal precipitation below 900m asl are more favourable for clay  
416 illuviation, which brings higher BS (>50%). Whereas, the lower temperature and higher  
417 precipitation at elevations above 900m asl hamper the percolation of water through cracks in the  
418 soil, pathway of downward transportation of clay minerals. The lower temperature and more moist  
419 soils due to the high rainfall limit the formation of cracks via shrinking process in clay-rich soils.  
420 Similar to many studies (Sevgi and Tecomen, 2009; Chuai et al., 2012; and Vogel and Märker,  
421 2011), positive correlations between SOM and elevation were found below 900m asl in most rock  
422 types. These values became negative above this elevation line due to a lower clay content found  
423 in soils at this elevation range.

### 424 ***5.3. Relief***

425 Slope inclination, position and form play remarkable roles in the variability of soil properties and  
426 occurrences of certain soil types Clemens et al., 2010; Cong, 2011; Qin et al. 2009, 2012). In the  
427 monocropping culture of maize in Yen Chau, soils on steep slopes at a same slope position with a  
428 similar cultivation period have a remarkably lower topsoil thickness and SOM content than those

429 at gentler slopes. This problem was caused by soil erosion triggered by intensive cultivation  
430 activities.

431 In accordance with the findings of Clemens et al. (2010), soils at crest and upper slope positions  
432 tend to have higher SOM stocks commonly represented by Humic property. This is because forest  
433 invasion for agricultural land occurred last at these areas, hence younger cultivation periods and  
434 more soil carbon retained in the topsoil. Luvisols and Alisols mainly have Vertic, Nitic, Leptic and  
435 Profondic properties at the middle slope and Siltic property at the foot slope. The Leptic property  
436 of Luvisols and Alisols and Dystric property of Cambisols occur at a location that has a high slope  
437 gradient and convex form. This is where the topsoil is shallow because of severe soil erosion and  
438 a high stone content is found in the both topsoil and subsoil. When a soil has a shallower soil depth  
439 and a remarkably higher stone content, the soil then becomes Regosols or Leptosols. This is where  
440 Regosols and Leptosols were mainly found in Yen Chau. Similar to the findings of Schuler (2008),  
441 Clemens et al. (2010) and Häring et al. (2010), Siltic for Luvisols and Alisols and Luvic for  
442 Cambisols are the major properties in the foot slope position for the deposition of soil particles  
443 eroded from upper slope positions.

444 In the agreement with Schuler (2008) and Clemens et al. (2010), the study found that the straight  
445 forms resulted in better soil structure, soil stability, less susceptibility to erosion and better  
446 retaining of soil carbon. Thus, soils at locations with straight forms had higher stocks of SOM in  
447 the topsoil than those at locations with the other forms. Locations with convex slopeforms at high  
448 slope gradients are more prone to erosion and were found to have shallowest topsoil and lowest  
449 SOM stocks. Concave forms were found to be either the result of natural formation or small  
450 landslides. In the first case, the topsoil can be deep and contain high SOM stocks because of the  
451 convergence shape that collects soil particles eroded from higher points, but can, at the same time,

452 result in small landslides due to weaker soil structure. In the latter case, the topsoil was removed  
453 and the subsoil is exposed, which resulted in low SOM stocks and poor crop growth. Overall,  
454 however, slopeform does not stand out for a very important variable of soil fertility which should  
455 rather depend more heavily on other factors such as parent material, elevation and cultivation  
456 period or the history of land use.

#### 457 **5.4. Biological activity, human impact and time**

458 Similar to findings of Clemens et al. (2010) and Häring et al. (2010, 2013a and 2013b), macro-  
459 organisms were seen most active in the topsoil within the depth of 10-30cm. Major burrowing  
460 animals were termites, ants, earthworms, crickets, and beetles whose activities help create space  
461 for microorganisms and root penetration, water infiltration, and turn over organic matter in the  
462 soil. These activities contributed to the intermediate horizon of AhBt or BtAh in between A and  
463 Bt horizons. An E-horizon was rarely found. Microorganisms play an important role in increasing  
464 organic matter content in the soil through physical and biochemical processes. As indicated by  
465 Häring et al. (2010, 2013a and 2013b), soils in undisturbed forest land of Yen Chau had deeper  
466 and darker topsoil than soils that were converted from forest to agriculture. These soils were  
467 Phaeozems developed on limestone.

468 The human impact, especially land-use change from forest to maize, effects the distribution of  
469 soils and their properties (Schuler, 2008). A remarkable difference between average SOM stocks  
470 in the topsoil of Phaeozems (20-27 kg/m<sup>2</sup>) and the other soils (2-14 kg/m<sup>2</sup>) well proved this fact.  
471 Häring et al. (2010) found a decline in soil organic matter by 66%, N<sub>t</sub> by 67%, exchangeable Ca<sup>2+</sup>  
472 by 91%, Mg<sup>2+</sup> by 94%, K<sup>+</sup> by 73%, available P by 75%, pH values by 2.2 units, and cation  
473 exchange capacity by 56%. Häring et al. (2013a) found a higher total SOC loss (6–32%), a lower  
474 decomposition (13–40%), and a lower SOC input (14–31%). In terms of the mass of soil loss in

475 Yen Chau, Tuan et al. (2014) estimated that the loss due to the current maize cropping practice by  
476 local farmers reached  $174 \text{ t ha}^{-1} \text{ a}^{-1}$ . Soil erosion over years at steep upper and middle slope  
477 positions turned Luvisols and/or Alisols into Regosols (Häring et al., 2010), and led to the  
478 formation of Cambisols at low to moderate foot slope positions (Clemens et al., 2010).

479 In regards to the factor time, the initial agricultural activity was mainly slash-and-burn and shifting  
480 cultivation in mountainous regions of Vietnam, which was stated to be sustainable (Dao, 2000;  
481 Vien et al., 2004) and did not change much the nature of the soils. The population growth over the  
482 last decades led to increasing demands on food and forests were tremendously taken for  
483 agriculture. Since this time, soils of Yen Chau have been changed forever (Häring et al., 2013a;  
484 Häring et al., 2013b; Tuan et al., 2014).

## 485 **6. Conclusion**

486 This paper applies a fuzzy soil mapping approach to derive fuzzy similarity functions in an effort  
487 to develop soil and soil fertility maps for a region in NW Vietnam. These functions are constructed  
488 from descriptive knowledge represented by environmental factors that have impacts on soil  
489 occurrences and soil fertility variations. To best describe the distinctive extreme relief  
490 characteristic of the study area, a detailed 29 fuzzy slopeform system was formulated and  
491 constructed on a hypothesis that spatial distribution of soils and their fertility degrees could be  
492 better achieved from this parameter. From the results of the study, the following conclusions are  
493 made:

494 1) The system of 29 fuzzy slopeforms was successfully developed from five major slope  
495 positions. This parameter well delineates available surface forms of hill slopes from mountain  
496 tops to valleys, which allows the possibility to predict the occurrence of a soil and assess its  
497 fertility status at any location within the area of 10m by 10m.

- 498 2) We were able to formulate the soil-environmental relationship based on the soil data acquired  
499 and soil fertility classes calculated for the mapping area. This confirms the ability of this soil  
500 mapping approach in obtaining descriptive knowledge for digital soil mapping of an area with  
501 limited or no soil information (Zhu et al., 2010).
- 502 3) Good map accuracies of the RSG map and the soil subunit map (76% and 72%, respectively)  
503 reveal the applicability of the 29 fuzzy slopeform system in digital soil mapping for areas with  
504 extreme relief conditions like the one in this research. On the contrary, the validation of the  
505 soil fertility map shows just an average accuracy value of 60%. This is because:
- 506 4) Soil fertility does not vary strongly with the change in the surface form. Instead, land-use age  
507 after deforestation has been found to have a greater impact on soil fertility decline in Yen Chau  
508 district (Häring et al., 2010; Häring et al., 2013a; Häring et al., 2013b). For instance, the  
509 knowledge of cultivation period acquired from farmer interviews put in comparison with the  
510 analytic data for soil fertility control reveals that soils at upper slope positions tend to be more  
511 fertile than those at lower slope positions for having a younger period of cultivation due to  
512 forest clearance for agriculture happened from the bottom. The quantification of this  
513 information in better capturing soil fertility using this fuzzy mapping approach, therefore,  
514 should create an interesting research topic for this area in the future.

## 515 **Acknowledgements**

516 We would like to thank the local authorities of Yen Chau district and communes of Chieng Dong,  
517 Chieng On, Chieng Tuong, Chieng Sang, and Yen Son for providing useful information and close  
518 cooperation. We thank Andrea Zipp and Dr. Ludger Herrmann for doing and organizing laboratory  
519 analyses, and Hannah Kuhfeld for her help in improving the manuscript, and numerous farmers in  
520 Yen Chau for their field assistance, especially Lo Van Ha and Hoang Van Vui.



521 We wish to thank the German Science Foundation (DFG) (SFB 564) for the financial support  
522 within the framework of the SFB 564 “Research for sustainable land use and rural development in  
523 mountainous regions of Southeast Asia”.

524 Special thanks go to Prof. A-Xing Zhu, University of Wisconsin, and Prof. Qin Cheng-Zhi,  
525 Chinese Academy of Sciences for their free and helpful discussions and kind technical support.

#### 526 **Appendix a. Supplementary data**

527 Supplementary data associated with this article can be found in the online version  
528 <http://dx.doi.org/10.1016/j.catena.2017.03.01>. These data include Google maps of the most  
529 important areas described in this article.

#### 530 **References**

531 Bao, N. X. (ed.), 2004. Geology and mineral resources map of Vietnam, (F-48-XXXVII), scale  
532 1:200.000, department of geology and mining, Vietnam, Hanoi. 145 pp.

533 Batjes, N.H., 2008. Mapping soil carbon stocks of Central Africa using SOTER. *Geoderma* 146,  
534 58–65.

535 Bui, E.N. Loughhead, A., Corner, R., 1999. Extracting soil landscape rules from previous soil  
536 survey, *Sutr. J. Soil Res.* 37, 495–508.

537

538 Burrough, P.A., 1989. Fuzzy mathematics methods for soil survey and land evaluation. *Journal of*  
539 *Soil Science* 40, 447–492.

540 Burrough, P.A., 1996. Natural objects with indeterminate boundaries. In: Burrough, P.A., Frank,  
541 A.U. (Eds.), *Geographic Objects with Indeterminate Boundaries*. Francis and Taylor,  
542 London. 365pp.

543 Chuai, X.W., Huang, X.J., Wang, W.J., Zhang, M., Lai, L. and Liao, Q.L., 2012. Spatial variability  
544 of soil organic carbon and related factors in Jiangsu Province, China. *Pedosphere* 22(3),  
545 404–414.

546 Clemens, G., Fiedler, S., Cong, N.D., Dung, N.D., Schuler, U., Stahr, K., 2010. Soil fertility  
547 affected by land use history, relief position and parent material under tropical climate in  
548 NW-Vietnam. *Catena* 81, 87-96.

549 Conarcher, A.J., Dalrymple, J.B., 1997. The nine unit landsurface model: an approach to  
550 pedogeomorphic research. *Geoderma* 18, 1–154.

551 Cong, N. D., 2011. SOTER database for land evaluation procedure: A case study in two small  
552 catchments of Northwest Vietnam. *Hohenheimer Bodenkundliche Hefte*, 101, Hohenheim  
553 University, Germany.

554 Douglas, D., Peucker, T., 1975. Detection of Surface-Specific points by Local Parallel Processing  
555 of Discrete Terrain Elevation Data, *Computer Graphics, Visions and Image Processing*.  
556 Vol.4, No.2 pp. 375–387 (December 1973).

557

558 FAO, 2006. *Guidelines for Soil Description*, 4<sup>th</sup> edition. Rome, Italy. 97pp.

559 Häring, V., Clemens, G., Sauer, D., Stahr, K., 2010. Human-induced soil fertility decline in a  
560 mountain region in Northern Vietnam. *Die Erde* 150, Berlin, Special Issue “Fragile  
561 Landscapes”, 235–253.

562 Häring, V., Fischer, H., Cadisch, G., Stahr, K., 2013a. Implication of erosion on the assessment of  
563 decomposition and humification of soil organic carbon after land use change in tropical  
564 agricultural systems. *European Journal of Soil Science*.

565 Häring, V., Fischer, H., Cadisch, G., Stahr, K., 2013b. Improved  $\delta^{13}\text{C}$  method to assess soil  
566 organic carbon dynamics on sites affected by soil erosion. *Soil Biology & Biochemistry*  
567 65 (2013) 158–167.

568 Herrmann, L., Graef, F., Wellwe, U., Stahr, K., 2001. Land use planning on the basis of  
569 geomorphic units: experiences with the SOTER approach in Niger and Benin. *Z.*  
570 *Geomorph. N. F.* 124, 111–123.

571 IUSS Working Group WRB, 2006. World reference base for soil resources 2006, 2nd ed. World  
572 Soil Resources Report, No. 103. FAO, Rome.

573 Jahn, R., Blume, H.P., Asio, V.B., 2003. Students guide for soil description, Soil classification and  
574 site evaluation. Universität Halle. 120 pp.

575 Jenny, H., 1941. Factors of soil formation: A system of quantitative pedology. McGraw-Hill, New  
576 York. 281 pp.

577 Mausbach, J.M., Seybold, C.A., 1998. Assessment of soil quality. In: Lal, R. (Ed.), *Soil Quality*  
578 *and Agricultural Sustainability*. Sleeping Bear Press, Chelsea, USA.

579 McBratney, A.B., Medonça Santos, M.L., Minasny, B., 2003. On digital soil mapping. *Geoderma*,  
580 117, 3–52.

581 Odeh, I.O.A., 1991. Elucidation of soil-landform inter-relationships by canonical ordination  
582 analysis. *Geoderma* 49, 1–32.

583 Parton, W.J., Schimel, D.S., Cole, C.V., Ojima, D.S., 1987. Analysis of factors controlling soil  
584 organic matter levels in Great Plains grasslands. *Soil Science Society of America Journal*  
585 51, 1173–1179.

586 Qi, F., Zhu, A.X., 2003. Knowledge discovery from soil maps using inductive learning.  
587 *International Journal of Geographical Information Science* 17, 771–795.

- 588 Qin, C.Z., Zhu, A.X., Shi, X., Li, B.L., Pei, P., Zhou, C.H., 2009. The quantification of spatial  
589 gradation of slope positions. *Geomorphology* 110, 152–161.
- 590 Qin, C.Z., Zhu, A.X., Qiu, W.L., Lu, Y.J., Li, B.L., Pei, T., 2012. Mapping soil organic matter in  
591 small low-relief catchments using fuzzy slope position information. *Geoderma* 171–172,  
592 64–74.
- 593 Qin, J.H., Wang, Q., Sung, H., 2013. Changes of organic carbon and its labile fractions in topsoil  
594 with altitude in subalpine-alpine area of southwestern China. *Acta Ecol. Sin.* 33, 5858–  
595 5864.
- 596 Schuler, U., 2008. Towards regionalisation of soils in northern Thailand and consequences for  
597 mapping approaches and upscaling procedure. *Hohenheimer Bodenkundliche Hefte*, 89,  
598 Hohenheim University, Germany.
- 599 Schuler, U., Herrmann, L., Ingwersen, J., Erbe, P., Stahr, K., 2010. Comparing mapping  
600 approaches at subcatchment scale in northern Thailand with emphasis on the Maximum  
601 Likelihood approach. *Catena* 81, 137–171.
- 602 Sevgi, O., Tecomen, H.B., 2009. Physical, chemical and pedogenetical properties of soil in relation  
603 with altitude at Kazdagi upland black pine forest. *J Environ Biol* 30(3): 349–354.
- 604 Six, J., Feller, C., Deneff, K., Ogle, S.M., De Moraes Sa, J.C., Albrecht, A., 2002. Soil organic  
605 matter, biota and aggregation in temperate and tropical soils—effects of no-tillage.  
606 *Agronomie* 22, 755–775.
- 607 Skidmore, A.K., 1990. Terrain position as mapped from a gridded digital elevation model.  
608 *International Journal of Geographical Information Systems* 4(1), 33–49.

609 Speight, J.G., 1990. Landform, In: McDonald, R.C., Isbell, R.F., Speight, J.G., Walker, J.,  
610 Hopkins, M.S. (Eds.), Australian soil and land survey field handbook, (2<sup>nd</sup> edition). Inkata  
611 Press, Melbourne, pp. 9–57.

612 Tuan, V.D., Hilger, T., MacDonald, L., Clemens, G., Shiraishi, E., Vien, T.D., Stahr, K., Cadisch,  
613 G., 2014. Mitigation potential of soil conservation in maize cropping on steep slopes. *Field*  
614 *Crops Research* 156 (2014) 91–102.

615 Vågen T-G., Winowiecky, L.A., 2012. Mapping of soil organic carbon stocks for spatially explicit  
616 assessment of climate change mitigation potential. *Environ.Res.Lett* 8(1), 1–9.

617 Van Engelen, V.W.P., Wen, T.T., 1995. Global and national soils and terrain digital dabases  
618 (SOTER): Procedures manual, ISRIC, Wageningen, the Netherlands. 138pp.

619 Vien, T.D., Dung, N.V., Dung, P.T., Lam, N.T., 2004. A nutrient balance analysis of the  
620 sustainability of a composite swiddening agroecosystem in Vietnam’s northern mountain  
621 region. *Southeast Asian Studies*, Vol. 50, No. 4.

622 Vogel, S., Märker, M., 2011. Characterization of the pre-AD 79 Roman paleosol south of Pompeii  
623 (Italy): Correlation between soil parameter values and paleo-topography. *Geoderma* 160,  
624 548–558.

625 Willmott, C.J. (1984): On the evaluation of model performances in physical geography. In: Gaile,  
626 G.L., Willmott, C.J. (Eds.), *Spatial statistics and models*. D. Reiden Publi., Dordrecht, the  
627 Netherlands, pp. 43–460.

628 Winowiecki, L.A., Vågen T-G., Massawe, B., Jelinski, N.A., Lyamchai, C., Sayula, G., Msoka,  
629 E., 2015. Landscape-scale variability of soil health indicators: effects of cultivation on  
630 soil organic carbon in the Usambara Mountains of Tanzania. *Nutr Cycl Agroecosyst*. DOI  
631 10.1007/s10705-015-9750-1.

632 Yang, L., Zhu, A.X., Li, B.L., Qin, C.Z., Pei, T., Liu, B.Y., Li, R.K., Cai, Q.G., 2007. Extraction  
633 of knowledge about soil-environment relationship for soil mapping using fuzzy c-means  
634 (FCM) clustering. *Acta Pedol. Sin.* 44, 16–23.

635 Young, A., 1972. *Slopes*. Oliver & Boyd, Edinburgh, pp. 288.

636 Zhu, A.X., Band, L.E., Dutton, B., Nimlos, T.J., 1996. Automated soil inference under fuzzy logic.  
637 *Ecol. Modell* 90, 123–145.

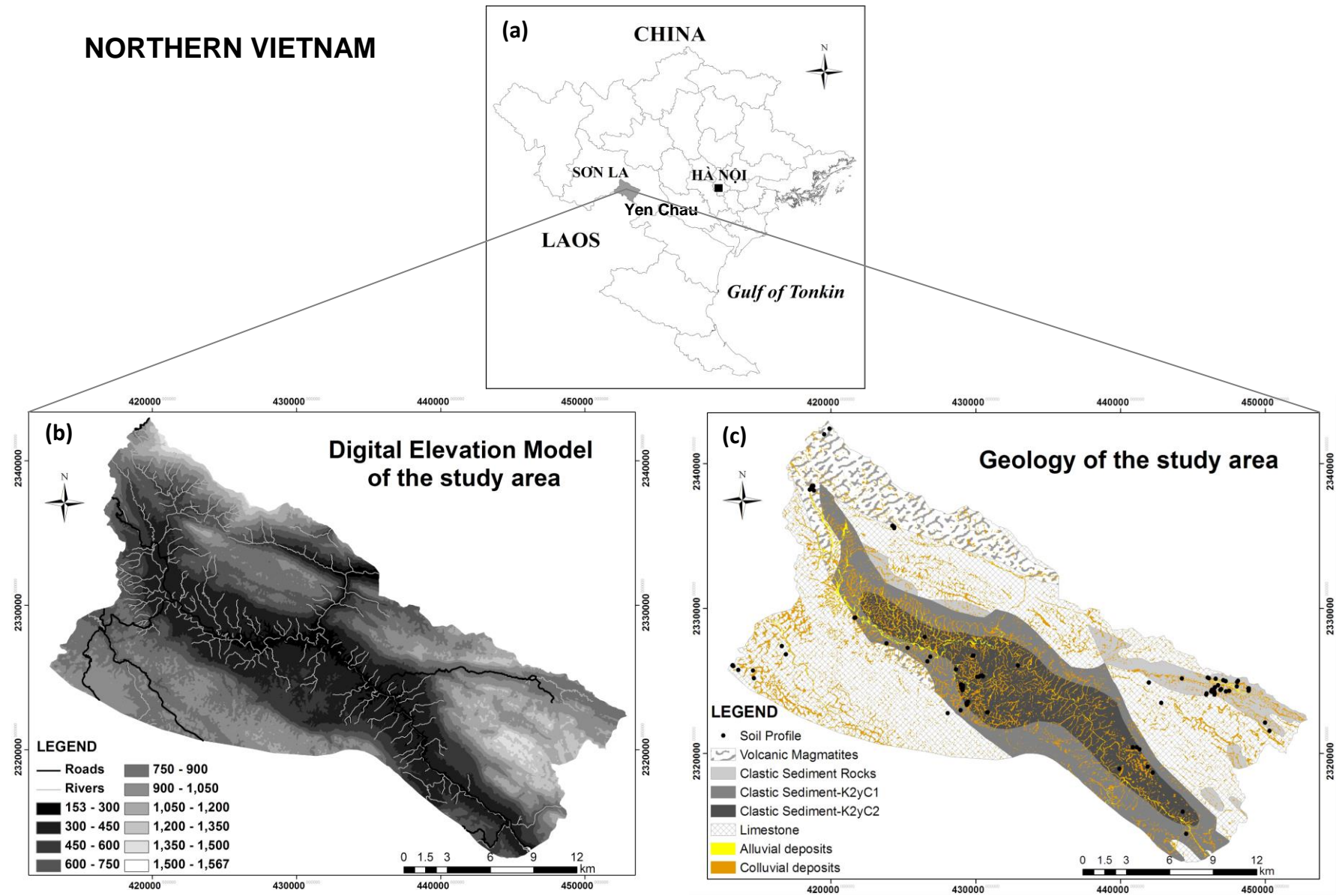
638 Zhu, A.X., 1997a: A similarity model for representing soil spatial information. *Geoderma*, 77,  
639 217–242.

640 Zhu, A.X., Band, L., Vertessy, R., Dutton, B., 1997b. Deriving soil property using a soil land  
641 inference model (SoLIM). *Soil Sci. Soc. Am. J.* 61:523–533.

642 Zhu, A.X., Yang, L., Li, B., Qin, C.Z., Pei, T., Liu, B., 2010. Construction of membership  
643 functions for predictive soil mapping under fuzzy logic. *Geoderma* 155, 164–174.

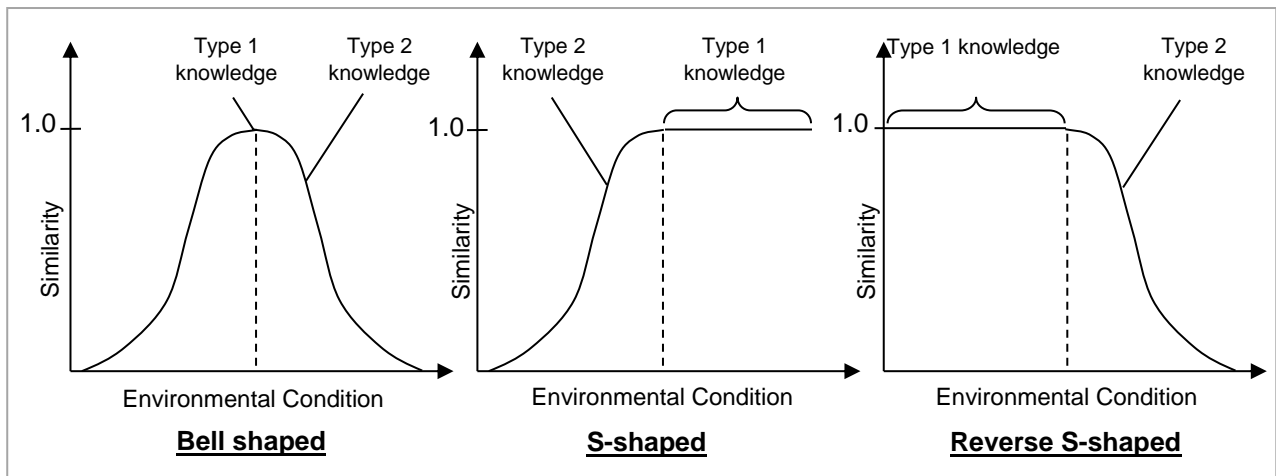
## LIST OF FIGURES

- Figure 1.** a) Geographic location of the study area in Yen Chau district, Son La province; b) The DEM of Yen Chau district; c) Geology of Yen Chau district and locations of soil profiles
- Figure 2.** The three basic forms of membership functions (Zhu et al., 1999)
- Figure 3.** Predicted soil map of a small area of the study area. The last four subsoil units (with blank colour patterns) are not found within this sample area, but characterized for the whole study area
- Figure 4.** Distribution of subsoil units along a slope for Luvisols
- Figure 5.** Predicted soil quality map of the study area (a), a 3D representation of major soil quality classes of a smaller area as example (b)
- Figure 6.** Variability of BS over different parent rocks and major soil groups
- Figure 7.** Locations of validation points



**Figure 1.** a) Geographic location of the study area in Yen Chau district, Son La province; b) The DEM of Yen Chau district; c) Geology of Yen Chau district and locations of soil profiles







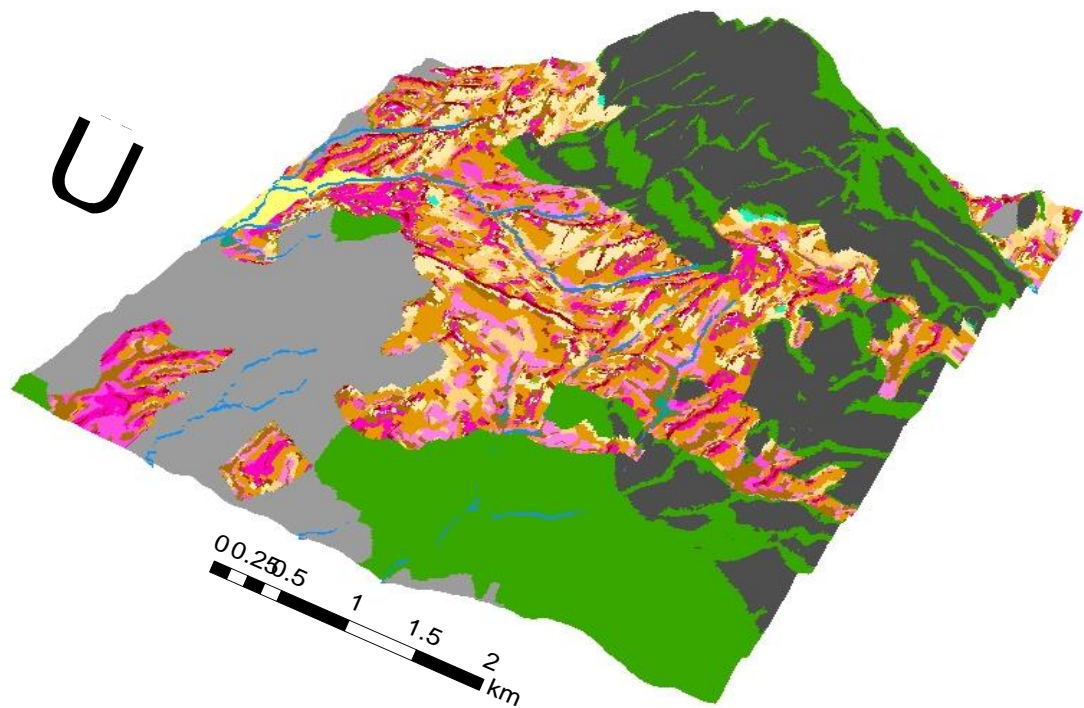




















**Figure 2.** The three basic forms of membership functions (Zhu et al., 1999)



**LEGEND - Reference Soil Groups with subsoil units**

 River	 Skeletic Regosols
 Cutanic-Humic Alisols	 Dystric Leptosols
 Cutanic-Profondic Alisols	 Luvic-Haplic Phaeozems
 Siltic Alisols	 Calcic-Siltic Fluvisols
 Cutanic-Leptic Alisols	 Anthrosols/Paddy
 Cutanic-Humic Luvisols	 Forest
 Cutanic-Profondic Luvisols	 Unmapped area
 Siltic Luvisols	 Cutanic-Nitic Luvisols
 Humic Cambisols	 Cutanic-Leptic Luvisols
 Dystric Cambisols	 Haplic-Chromic Vertisols
 Luvic Cambisols	 Vertic-Allic Stagnosols

**Figure 3.** Predicted soil map of a small area of the study area. The last four subsoil units (with blank colour patterns) are not found within this sample area, but characterized for the whole study area

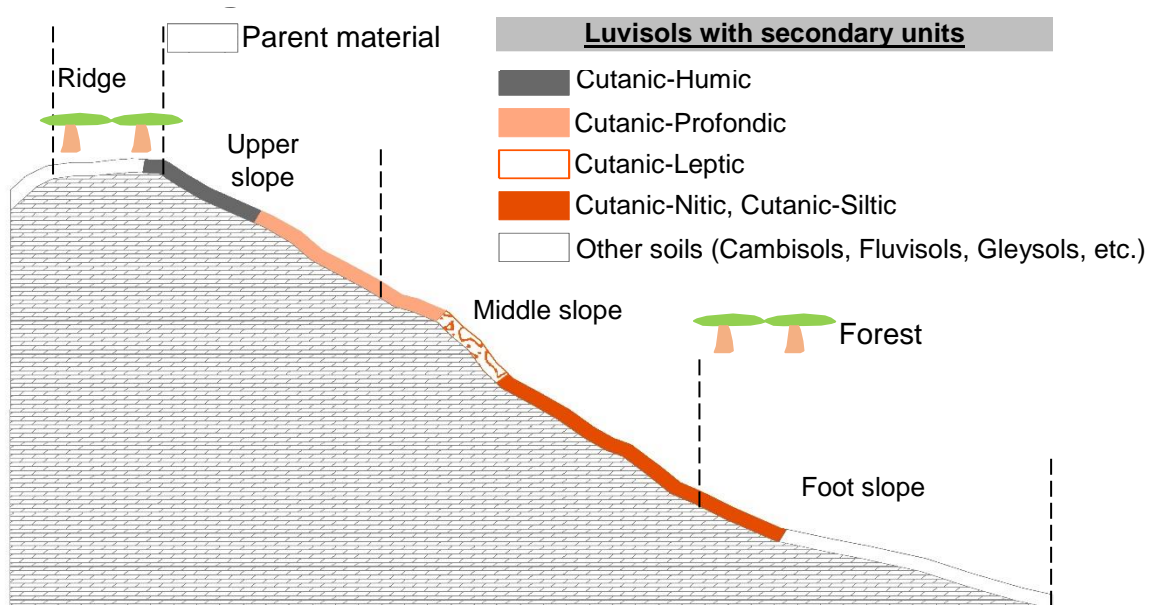


**Figure 4.** Distribution of subsoil units along a slope for Luvisols

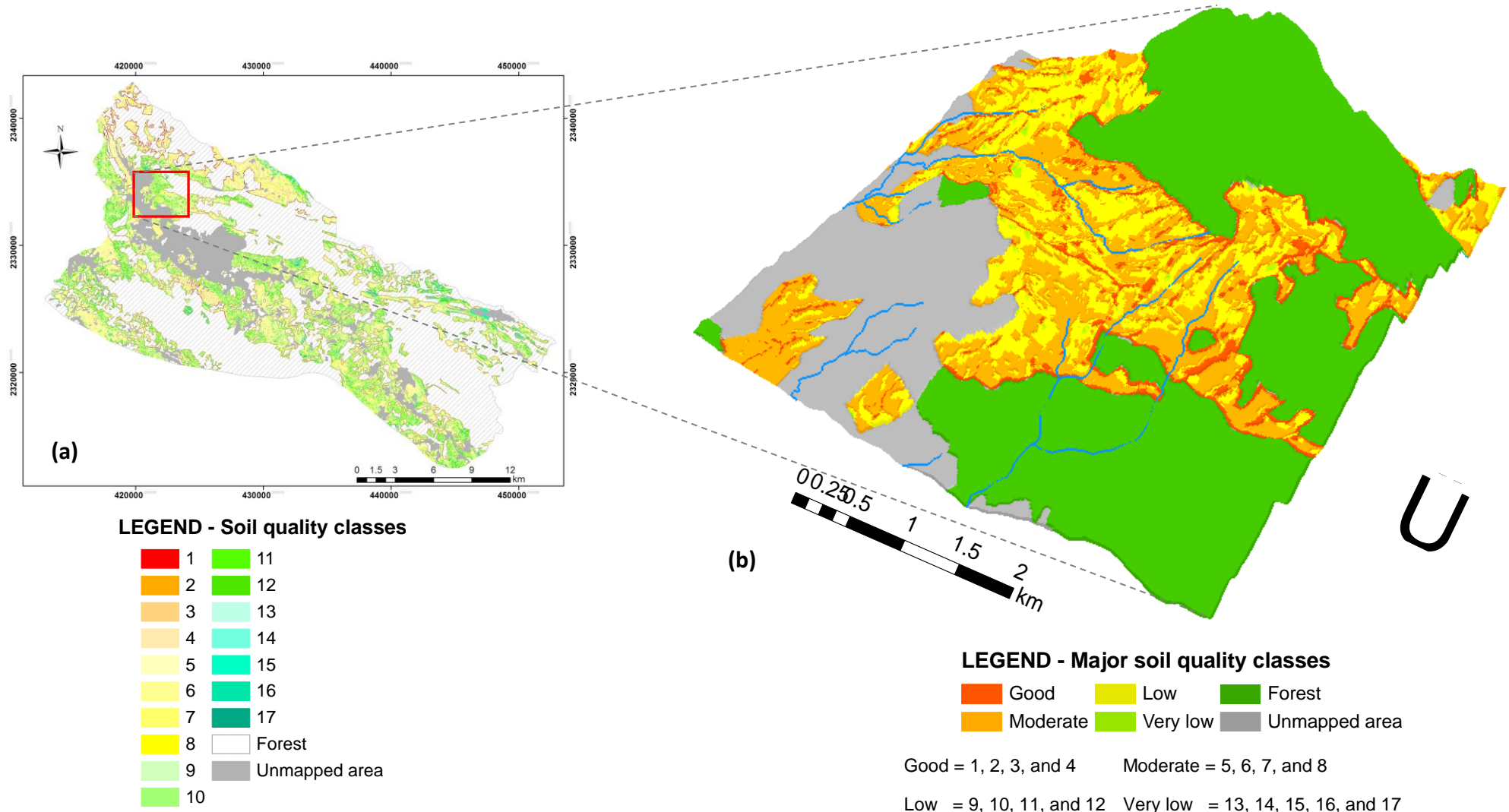


**Figure 5.** Predicted soil quality map of the study area (a), a 3D representation of major soil quality classes of a smaller are as example (b)

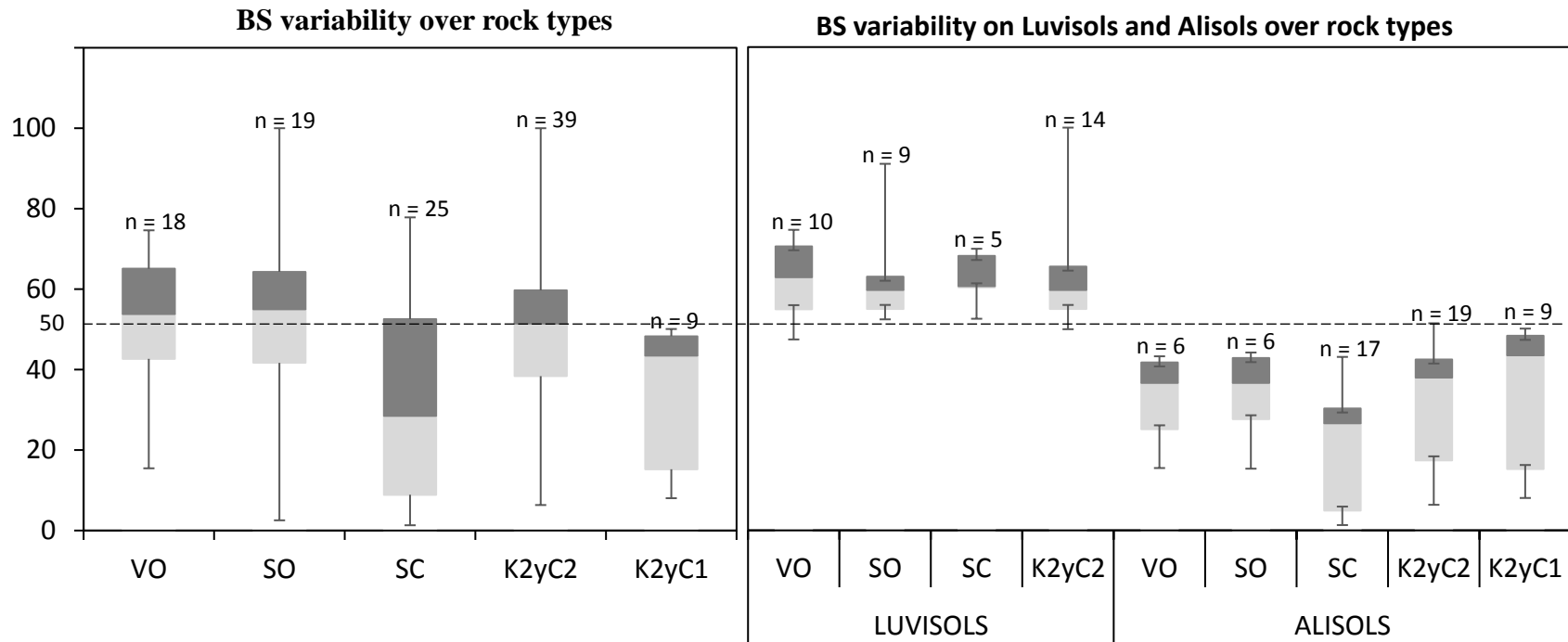


**Figure 6.** Variability of BS (%) for the ERS over different parent rocks and major reference soil groups

Explanation of the supplementary data in the .csv plot data files:

Luvisols = 1, Alisols = 2, VO = 1, SO = 2, SC = 3, K2yC2 = 4, K2yC1 = 5

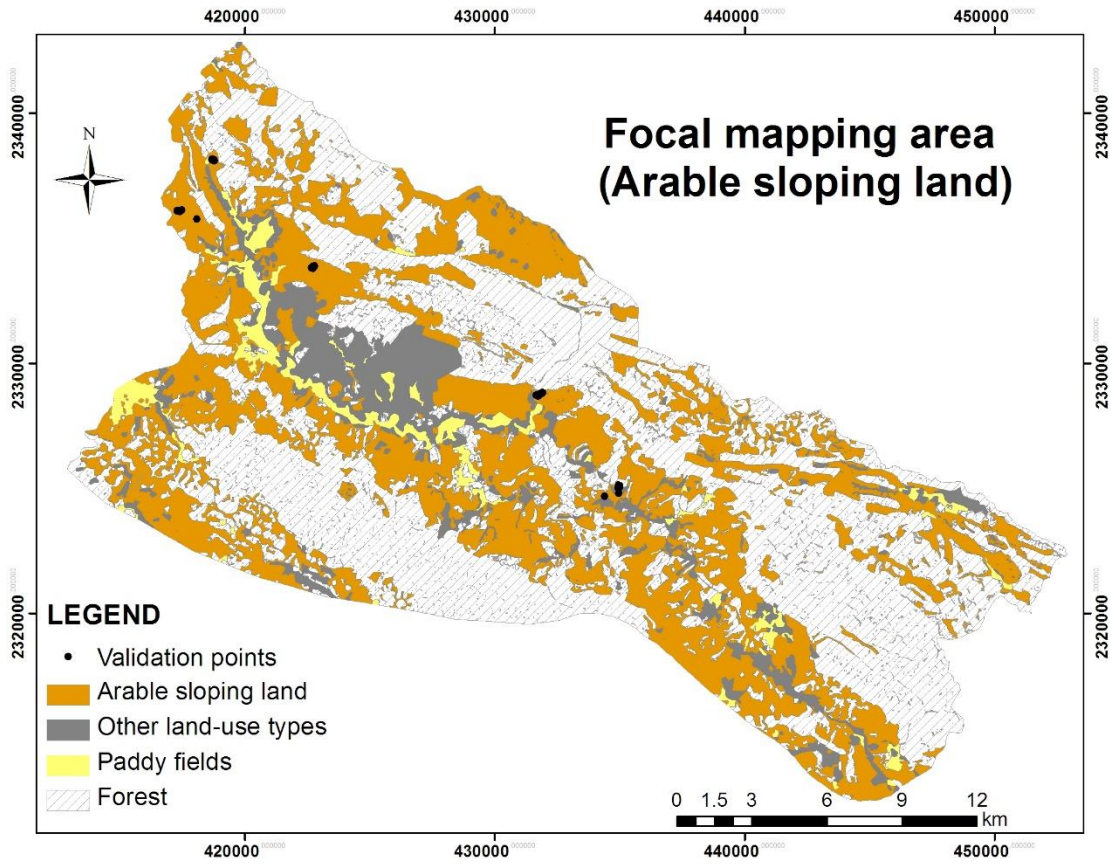


**Figure 7.** Locations of validation points